Computer Vision Techniques for Firebrand Detection and Characterization

Ali Tohidi, Michael Gollner
University of Maryland College Park, College Park, MD, USA

Christine Standohar-Alfano, Stephen Quarles
Insurance Institute for Business & Home Safety, Richburg, SC, USA

Abstract

One of the most important mechanisms for fire spread in the wildland urban interface (WUI) is the transport of firebrands. These small burning particles have been found to be responsible for more than half of home ignitions in WUI areas, however techniques to characterize their production and transport are limited. This study integrates various computer vision techniques to develop a novel particle tracking algorithm than can be used to quantify exposure from firebrand showers. Application of the algorithm to video from a full-scale burning test of a Leyland cypress tree through a wind field delivers promising results for the calculation of the number, surface area, and mass flux of generated firebrands.

Keywords: Firebrand, Wildfire, Particle Tracking, Image Processing

Introduction

Wildfires expose people, properties, and ecosystems to a pervasive threat, particularly at the Wildland-Urban Interface (WUI), where wildland (vegetation) and developed communities intermingle. There are now more than 47 million houses in the United States within WUI, putting people and properties at direct risk from wildfires [1]. Three pathways have been found that contribute to wildfire propagation through the WUI: radiative heating from the main fire front, direct flame contact from nearby flames, and spot fire ignition by firebrands. The first two mechanisms have been studied extensively in the literature [2–6], however, firebrands have been much less studied, despite their importance or even dominance in spreading WUI fires. Firebrand transport occurs when combusting elements from vegetation or structures break off and are lofted through the fire plume. Due to the fire plume's updraft, generated firebrands may travel high enough to be transported far downwind through the atmospheric boundary layer. There are several studies where firebrands' lofting and downwind

transport is investigated [7], however, due to the complexity of firebrand generation and transport, there is very little experimental knowledge of this phenomenon while firebrands are still in flight [1]. Therefore, it is crucial to develop measurement techniques that can quantify exposure from “showers” of multiple firebrands.

Numerous studies have captured firebrand number, mass, and area from both controlled and uncontrolled fires using water collection pans [8,9]. Observation of firebrands during transport, however, is much more limited [10,11]. Recently, Tohidi and Kaye [7] developed a particle tracking algorithm to capture the flight trajectory of non-combusting model firebrands during lofting and downwind transport through the velocity field of a jet in a cross-flow. The experimental results show that, unlike previous studies [5,12–15], lofting and downwind transport cannot be decoupled from one another, and that firebrands’ initial conditions, including release angle and height, significantly change the ground distribution and consequently spot fire ignition potential during wildfires. These results highlight the importance of in-flight tracking versus ground measurements.

In this study, a Particle Tracking Velocimetry (PTV) software was developed based on previous work by Tohidi and Kaye [7]. This diagnostic tool used standard optical cameras to deliver a quantified firebrand flux from experiments of burning vegetative fuels under wind-driven conditions in terms of number and mass. This data is necessary to quantify a WUI hazard scale, support code development and model validation, and provide insights on the influence of various exposure scenarios.

Experimental Setup

Experiments were conducted in a large scale wind tunnel testing facility at the Insurance Institute for Business & Home Safety (IBHS) Research Center. A 1.5 m tall Leyland cypress tree, *Cupressus × leylandii*, was horizontally oriented parallel to a fluctuating wind with 5.4 m/s average velocity, as shown in Fig. 1, and ignited with a gas-fed star-shaped burner at the base. The horizontal orientation was necessary to provide uniform and repeatable ignition conditions. The burner was removed from the base after complete ignition of the tree. After ignition, the test ran for approximately 5 minutes, at which time the tree had burned down and no firebrands were being generated. The entire process was recorded using a Sony DSC-RX10 II camera from the side view. The captured video is used to track and quantify the firebrand generation process from the tree utilizing a particle tracking algorithm.

Methodology

The developed algorithm uses commercially available digital (action) cameras. Effective use of such cameras necessitates careful characterization of the imaging sensors. The imaging distortions, due to

a fish-eye effect, are measured and corrected by an *Omnidirectional Camera Calibration* algorithm; see [16]. The pixel ratio of the image space is characterized using available scale parameters in the image, i.e. white stripes on the background, and the focal point from the tree. Then, the PTV package is utilized to detect and count the generated firebrands.

Fig. 1. (Left) A horizontally oriented tree before burning by a star-type gas burner from the left through the wind tunnel boundary layer, and (right) generated firebrands from the same burning tree.

Accurate estimation of the number and surface area (size) of firebrands will depend on the field of view and distance from the cameras. The utilized commercial camera supports video at resolutions as high as 1920×1080 pixels with three color channels, which corresponds to approximately 0.12 mm resolution within the field of view. Given that previous experimental studies [8] on firebrands produced by natural fuels have found that the smallest dimension of a firebrand was commonly 3-4 mm, the dimensions of firebrands will, generally, be resolved with less than 10% error under these conditions. This error margin was much smaller than the current methods that are being used for measurement and estimation of the number of firebrands [17].

Resolving small moving objects from videos or image pairs is commonly called Particle Tracking Velocimetry (PTV). This technology is well documented in the field of experimental fluid dynamics [18], [19]. The most challenging aspect of particle tracking is the detection of particles through the image space. To this end, a combination of various image segmentation techniques, i.e. flame masking, background subtraction, and field averaging, was used. After separation of the foreground from the background, conventional edge detection methods, such as the Marr-Hilderth method [20] was utilized to identify firebrands (blobs) and make the image ready for thresholding and intensity adjustment procedures. As shown in Fig. 2, a set of mathematical morphology algorithms such as Erosion and Dilation operations [10] was used to recognize the shape of firebrands and calculate their corresponding geometric properties based on the form and number of occupying pixels in the image. This provided the projected surface area of firebrands that was used in conjunction with the available correlation with mass ($s \sim m^{2/3}$, see [21]) to calculate the mass flux.

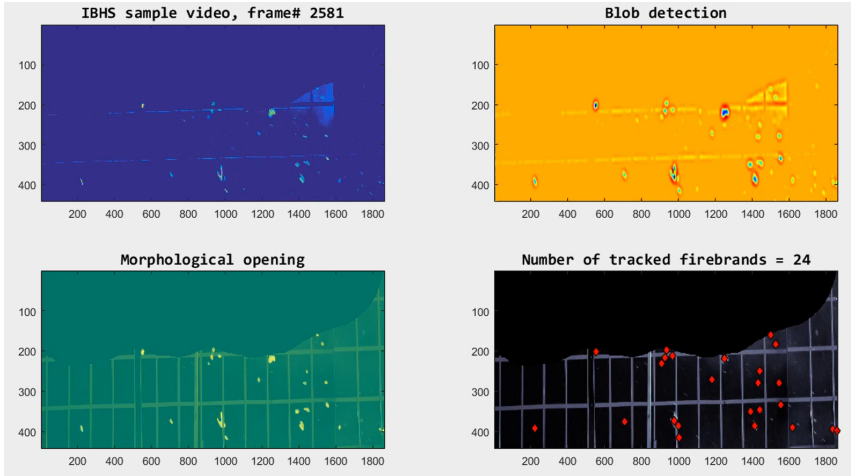

Fig. 2. Implementation of the developed PTV algorithm on recorded videos. The solid black area is the masked burning tree, and the red dots are the resolved (detected) firebrands.

Results and Discussions

To quantify the detection process, a horizontally oriented band across the test region with a very narrow width (5 mm) was considered as the control volume. This control volume, outlined by red lines, as well as the time-history signature of detected firebrands through the image space are shown in Fig. *3*.

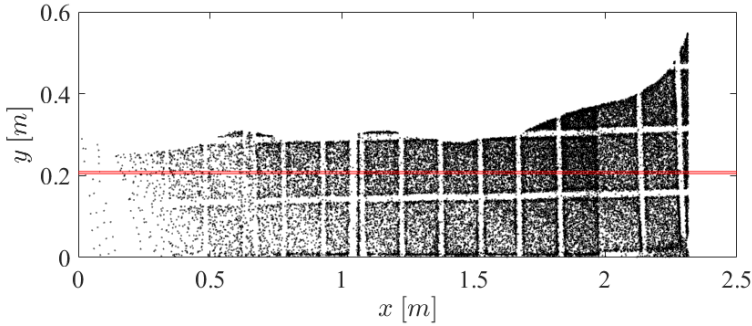

Fig. 3. Shown is the time-history signature of the resolved firebrands through the image space. Also, the 5 mm space between the red lines is the designated control volume. The large white area is the masked burning tree and vertical and horizontal stripes are from the background.

The number of firebrands that passed through the control volume was measured through 50 seconds of video. The control volume was also divided into 3 stations along the horizontal direction to quantify the spotting distribution as a function of horizontal distance, which

corresponded to water collection pans on the floor. Stations 1, 2 and 3 were then between 0-0.83 m, 0.83-1.67 m, and 1.67-2.5 m, respectively, from the origin of image space shown in Fig. *3*. Utilizing a counting algorithm, the number of observed firebrands along with their corresponding projected surface area was calculated within the control volume through time. Having these values and using the correlation between mass and surface area of firebrands, namely $m \sim s^{3/2}$ [21], it is possible to also estimate the number and mass flux, as shown in Fig. *4*.

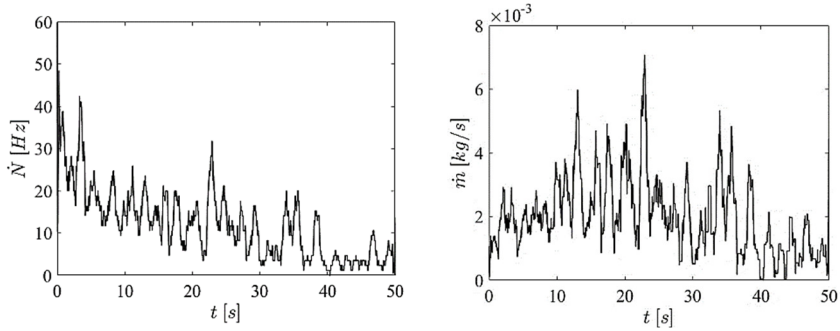

Fig. 4. (Left) frequency of the observed firebrands within the control volume; (Right) estimated mass flux using correlations from [21].

The number of detected firebrands increased drastically once the observation began. After approximately 5 s, a decreasing trend in number flux with sporadic spikes in time was evident. The observed spikes corresponded to the stochastic nature of the firebrand generation process. This was also the case for the estimated mass flux. The larger spikes were due to the release of large parts of the tree seen throughout the burning process. However, the largest estimated mass flux from the entire tree was still slightly less than 7 g/s. Integration of fluxes through time (50 s) leads to the total number of observed firebrands, 638, which was equivalent to an estimated 101 g. The estimated value of the mass was on the order of the obtained experimental mass, that was 166.2 g, which was collected using water-filled pans within the first 1.56 m downstream. The first order relative error of this case was 39.2 %. A large part of this error was because many of the firebrands traveled through the wind field and landed on the collecting pans before or after passing through the control volume. Hence, the lower estimated mass. In addition, the experimental mass was averaged over 3 repetitions without associated errors calculated between tests.

Further, it is possible to calculate the mass distribution along the horizontal direction within each station. Fig. *5*. shows the estimated cumulative mass of firebrands within each designated station. Based on Fig. *5*-left, most of the firebrands' mass was captured at the end of the domain, which signified the effect of horizontal wind. Also, the

probability density function (PDF) distributions, Fig. *5*-right, suggested that the probability of collecting firebrands with a mass greater than 6-8 g was higher for stations 2 and 3. The PDFs of station 2 and 3, however were very similar. In this regard, the probability of collecting small firebrands with mass less than 6 g was higher in station 1. This suggested that such firebrands may not be aerodynamically efficient to become lofted through the velocity field. Therefore, most experience a free-fall through their trajectory and do not get lofted far downstream. This observation was consistent with previous studies [6,22] where a minimum loftable size and mass were defined for firebrands.

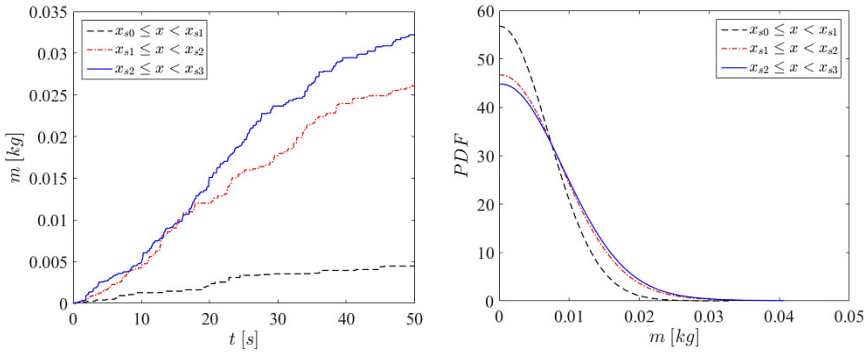

Fig. 5. Shown are cumulative mass (left) and probability density function (PDF) of the total estimated mass per time, within each station along the control volume (right). Through the control volume along the horizontal direction, $x_{s0} = 0\ m, x_{s1} = 0.83\ m$, $x_{s2} = 1.67\ m$, and $x_{s3} = 2.5\ m$.

Conclusions

A PTV algorithm was developed to investigate stochastic processes of firebrand generation. The algorithm was applied to an experimental case where a Leyland cypress tree was burned in a wind field. While the configuration shown may not be a completely accurate representation of the processes within a full-scale spreading WUI fire, it provided a repeatable configuration to determine the influence of wind and fuel type on the generation of firebrands. Application of the algorithm on captured video of the experiments allowed for calculating the number, surface area, and mass flux of the firebrands. The estimated cumulative mass flux by the PTV algorithm was on the order of the collected experimental mass. Future experiments with a wider field of view and associated errors in measured mass flux will help to validate this technique. The results, however, signify not only the potential of computer vision techniques for use in controlled wildland fire experiments, but also the potential to use these low-cost techniques in the field for quantification of firebrand exposure under relevant fire conditions.

Acknowledgements

Experiments were conducted at the IBHS Research Center with support from the USDA Forest Service through cooperative agreement 15-CA-11272167-058 funded through the Joint Fire Science Program award 15-1-04-4.

References

[1] S.E. Caton, R.S.P. Hakes, D.J. Gorham, A. Zhou, M.J. Gollner, *Review of Pathways for Building Fire Spread in the Wildland Urban Interface Part I: Exposure Conditions*, Fire Technol. 53 (2017) 429–473. doi:10.1007/s10694-016-0589-z.

[2] F. Albini, *Spot fire distance from burning trees: a predictive model*, USDA INT-56.U.S. Intermountain Forest and Range Experiment Station, 1979.

[3] F.A. Albini, I. Forest, *Potential spotting distance from wind-driven surface fires*, US Department of Agriculture, Forest Service, Intermountain Forest and Range Experiment Station, 1983.

[4] C.S. Tarifa, P.P. Del Notario, F.G. Moreno, *On the flight paths and lifetimes of burning particles of wood*, Symp. Combust. 10 (1965) 1021–1037. doi:10.1016/S0082-0784(65)80244-2.

[5] S.D. Tse, A.C. Fernandez-Pello, *On the flight paths of metal particles and embers generated by power lines in high winds—a potential source of wildland fires*, Fire Saf. J. 30 (1998) 333–356.

[6] E. Koo, P.J. Pagni, D.R. Weise, J.P. Woycheese, *Firebrands and spotting ignition in large-scale fires*, Int. J. Wildl. Fire. 19 (2010) 818. doi:10.1071/WF07119.

[7] A. Tohidi, N.B. Kaye, *Comprehensive wind tunnel experiments of lofting and downwind transport of non-combusting rod-like model firebrands during firebrand shower scenarios*, (2017). doi:10.1016/j.firesaf.2017.04.032.

[8] S.L. Manzello, A. Maranghides, W.E. Mell, *Firebrand generation from burning vegetation*, Int. J. Wildl. Fire. 16 (2007).

[9] S. Suzuki, S.L. Manzello, Y. Hayashi, *The size and mass distribution of firebrands collected from ignited building components exposed to wind*, Proc. Combust. Inst. (2012).

[10] A. Filkov, S. Prohanov, E. Mueller, D. Kasymov, M. El Houssami, J. Thomas, et al., *Investigation of firebrand production during prescribed fires conducted in a pine forest*, Proc. Combust. Inst. (2016) 1–11.

[11] M. El Houssami, E. Mueller, A. Filkov, J.C. Thomas, N. Skowronski, M.R. Gallagher, et al., *Experimental procedures characterising firebrand generation in wildland fires*, Fire Technol. 52 (2016) 731–751.

[12] N. Sardoy, J.-L. Consalvi, B. Porterie, A. Kaiss, *Transport and combustion of Ponderosa Pine firebrands from isolated burning trees*, in: 2006 1st Int. Symp. Environ. Identities Mediterr. Area, ISEIM, July 9, 2006 - July 12, Inst. of Elec. and Elec. Eng. Computer Society, Corte-Ajaccio, France, 2006: pp. 6–11.

[13] N. Sardoy, J.-L. Consalvi, B. Porterie, A. Fernandez-Pello, *Modeling transport and combustion of firebrands from burning trees*, Combust. Flame. 150 (2007) 151–169.

[14] N. Sardoy, J.L.L. Consalvi, a. Kaiss, a. C.C. Fernandez-Pello, B. Porterie, a.C. Fernandez-Pello, *Numerical study of ground-level distribution of firebrands generated by line fires*, Combust. Flame. 154 (2008) 478–488. doi:10.1016/j.combustflame.2008.05.006.

[15] E. Koo, R.R. Linn, P.J. Pagni, C.B. Edminster, *Modelling firebrand transport in wildfires using HIGRAD/FIRETEC*, Int. J. Wildl. Fire. 21 (2012) 396. doi:10.1071/WF09146.

[16] D. Scaramuzza, A. Martinelli, R. Siegwart, *A flexible technique for accurate omnidirectional camera calibration and structure from motion*, in: Fourth IEEE Int. Conf. Comput. Vis. Syst., 2006: p. 45.

[17] M. El Houssami, J.C. Thomas, A. Lamorlette, D. Morvan, M. Chaos, R. Hadden, et al., *Experimental and numerical studies characterizing the burning dynamics of wildland fuels*, Combust. Flame. 168 (2016). doi:10.1016/j.combustflame.2016.04.004.

[18] H.G. Maas, A. Gruen, D. Papantoniou, *Particle tracking velocimetry in three-dimensional flows*, Exp. Fluids. 15 (1993) 133–146.

[19] J. Westerweel, *Fundamentals of digital particle image velocimetry*, Meas. Sci. Technol. 8 (1997) 1379.

[20] D. Marr, E. Hildreth, *Theory of Edge Detection*, Proc. R. Soc. London B Biol. Sci. 207 (1980) 187–217. doi:10.1098/rspb.1980.0020.

[21] A. Tohidi, N. Kaye, W. Bridges, *Statistical description of firebrand size and shape distribution from coniferous trees for use in Metropolis Monte Carlo simulations of firebrand flight distance*, Fire Saf. J. 77 (2015) 21–35. doi:10.1016/j.firesaf.2015.07.008.

[22] S. Bhutia, M.A. Jenkins, R. Sun, *Comparison of firebrand propagation prediction by a plume model and a coupled–fire/atmosphere large–eddy simulator*, J. Adv. Model. Earth Syst. 2 (2010) 4. doi:10.3894/JAMES.2010.2.4.